JTTEE5 22:1358–1365
DOI: 10.1007/s11666-013-9961-4
1059-9630/$19.00 © ASM International

Peer Reviewed

Determination of Interfacial Fracture Toughness of Thermal Spray Coatings by Indentation

Yasuhiro Yamazaki, Masayuki Arai, Yukio Miyashita, Hiroyuki Waki, and Masato Suzuki

(Submitted March 5, 2013; in revised form June 10, 2013)

Adhesion is an important and basic property for thermal spray coatings. The standard tensile test method "ISO 14916" is usually used to evaluate the adhesive strength of coatings. On the other hand, the indentation test method has some advantages to evaluate the interfacial fracture toughness as the adhesive strength, arising from the following reasons: the test procedure and the specimen preparation are easy in comparison with the typical testing method. Collaborative research has been conducted by "Committee on Standard Development" in the Japan Thermal Spray Society to establish a standard test method for evaluating interfacial fracture toughness of thermal spray coatings using a conventional Vickers indenter. This article reports the differences among collaborators in round-robin tests performed in this committee and discusses the validity of the test method and test conditions with respect to the test results and finite element analyses. Comparison among collaborators reveals that interfacial fracture toughness can be obtained with a small scattering from the indentation test under constraints found on the basis of the results.

Keywords indentation test, interfacial fracture toughness, thermal spray coatings, test standardization

1. Introduction

Thermal spray processes, such as air plasma spraying (APS) and high velocity oxy-fuel (HVOF) spraying, are deposition technologies that apply metallic or nonmetallic coatings to a substrate. The quantification of interfacial fracture toughness of thermal spray coatings is important for the following reasons: (a) quality assurance of thermal spraying, (b) product design and performance assessment of coatings, (c) quantitative understanding of the degradation of adhesion in service, and (d) lifetime assessment of the coated components. The adhesion strength of thermal spray coatings is usually measured in accordance with the tensile method specified by the International Standard "ISO 14916." However, ISO 14916 cannot be applied to evaluate a coating with adhesion strength higher than glue strength, which is used to prepare the tensile test specimens. The indentation method (Fig. 1) is promising for evaluating such high-adhesion-strength coatings. Therefore, this method can simply evaluate the adhesion strength of a coating over a wide range by means of a Vickers hardness tester, which is widely accepted and used in industries. The committee on standard development in the Japan Thermal Spray Society (JTSS) has conducted collaborative research to establish a standard test method for the classification of coating adhesion by means of a conventional Vickers indenter. This study enabled us to recently submit a new research proposal entitled "Classification method of adhesive strength by indentation" at the ISO organization. In addition, we are preparing another proposal for determining interfacial fracture toughness of thermal spray coatings using the same indentation method.

The interfacial fracture toughness can be expressed either as a stress intensity factor, with units of MN $m^{-3/2}$, or as a fracture surface energy, with units of J m^{-2}. When applied unqualified to thermal spray coatings, "interfacial fracture toughness" can have different expressions, but the physical meaning remains the same. To clarify the test method, "indentation interfacial toughness," K_{IFC}, is differently used from interfacial fracture toughness, K_{IFC}. K_{IFC} is obtained using Vickers hardness tester and is identified from the total length of cracks induced along the

This article is an invited paper selected from presentations at the 5th Asian Thermal Spray Conference (ATSC 2012) and has been expanded from the original presentation. ATSC 2012 was held at the Tsukuba International Congress Center, Ibaraki, Japan, November 26-28, 2012, and was organized by the Japan Thermal Spray Society and the Asian Thermal Spray Society.

Yasuhiro Yamazaki, Mechanical and Control Engineering, Niigata Institute of Technology, Niigata, Japan; **Masayuki Arai**, Mechanical Engineering, Tokyo University of Science, Jastushika-ku, Japan; **Yukio Miyashita**, Mechanical Engineering, Nagaoka University of Technology, Nagaoka, Japan; **Hiroyuki Waki**, Mechanical Engineering, Iwate University, Morioka, Japan; and **Masato Suzuki**, The National Institute of Advanced Industrial Science and Technology, Tsukuba, Japan. Contact e-mail: axel@mce.niit.ac.jp.

interface by indentation. Shorter cracks mean that the associated thermal spray coating has higher interfacial toughness or adhesion strength. To determine such an interfacial toughness for thermal spray coatings, different organizations use different test methods, and there is no standard method.

This article introduces the results of a collaborative investigation by the committee in JTSS to establish an indentation test for determining the interfacial fracture toughness of thermal spray coatings. This article reports on the differences among collaborators in the performed round-robin tests and discusses the validity of the test and test conditions with respect to the results and finite element (FE) analyses.

2. Coating Materials Tested in the Round-Robin Test

Ceramic and metal coatings were prepared for testing in the round-robin program. The details of the coating materials and spray processes are listed in Table 1. Conventional structural steels and aluminum alloys were used as substrates. All coating materials were sprayed onto plate-shaped substrates having length, width, and thickness of 100, 50, and 5 mm, respectively. After spraying, small coating pieces of length in the range of 20-30 mm and width 7 mm were cut from the coated substrate. To prevent damage due to polishing, coating pieces were embedded in a room-temperature curing epoxy resin. In this project, samples embedded in Bakelite resin (thermosetting-type) were also prepared to study the influence of resin properties, such as rigidity, on the test results. The Young's moduli of the epoxy and Bakelite resins were approximately, 5 and 10 GPa, respectively. The test surface (i.e., cross section of the coatings) was polished to a mirror surface before the indentation test.

A further advantage of embedding the specimens in resins for indentation test is that they can be grouped with specimens used for microstructure and hardness tests, which are also usually embedded in resins to prevent damage during polishing and to improve handling.

3. Interfacial Indentation Tests

Indentation tests have been used to determine the toughness of brittle bulk materials such as ceramics (Ref 1-10). Such techniques have the following advantages: the equipment is available in many laboratories; specimen preparation is relatively simple, requiring only a polished surface; and many data and statistics can be obtained using a small sample. Therefore, these tests are used to evaluate the interface fracture toughness between a coating and its substrate (Ref 11-23). The indentation test is based on the crack length along the interface, induced by a pyramidal Vickers diamond indenter, as shown in Fig. 2. Chicot and Lesage et al. have conducted

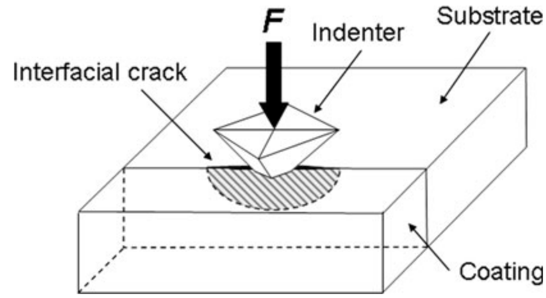

Fig. 1 Schematic illustration of an indentation test

systematic and extensive investigations to evaluate the interfacial fracture toughness (Ref 12-18). In the indentation test, the half-diagonal length of the impression (a), induced by indentation, increases with increasing applied load (test force). When a reaches a critical value, the interfacial crack is initiated from a corner of the impression and propagates along the interface with increasing applied load. Chicot and Lesage et al. have shown that the relationship between crack length (c) and applied load (F) can be represented as a straight line (called the crack curve) on a logarithmic scale for a given substrate and coating thickness (t) as shown in Fig. 3. The relationship between a and F is also linear (called the apparent hardness line), as shown in Fig. 3. The critical indentation load (F_c) and the corresponding crack length (c_c) define the visible interfacial crack initiation and are determined by the coordinates of the intersection points of both lines (Fig. 3). With the (F_c, c_c) couple, Chicot and Lesage et al. proposed the following equation to define the apparent interface toughness, K_{ca} (Ref 12).

$$K_{ca} = 0.015\left(\frac{E}{H}\right)_{I}^{1/2}\frac{F_c}{c_c^{3/2}}, \quad \text{(Eq 1)}$$

where $(E/H)_I^{1/2}$ is the square root of the ratio of the elastic modulus and the hardness at the interface. It is expressed as

$$(E/H)_I^{1/2} = \frac{(E_s/H_s)^{1/2}}{1+(H_s/H_c)^{1/2}} + \frac{(E_c/H_c)^{1/2}}{1+(H_c/H_s)^{1/2}}, \quad \text{(Eq 2)}$$

where E_i is the Young's modulus, H_i is the hardness, and subscripts s and c denote substrate and coating, respectively. Equation 2 can be obtained by considering the mean geometric features of the substrate and coating couple (Ref 12). If the residual stress in the coating is negligible, the crack curves intersect with the apparent hardness line at a unique point. This means that the obtained apparent interfacial toughness is independent of the coating thickness. Lesage and Chicot have also investigated the influence of residual stress in a coating on the interfacial cracking induced by indentation tests (15-18).

The abovementioned method is superior for evaluating the adhesion strength of coatings because the apparent interface toughness (P_c) can be obtained with sufficient accuracy, independent of the coating thickness. However, the method requires many indentation tests to determine

Table 1 Coating materials tested in the round-robin test

Coating specimen	Coating: Material	Coating: Spray process	Coating: Thickness (mm)	Bond coat	Substrate
Ceramic					
8YSZ-P	8YSZ (porous)	APS(a)	0.3, 0.6, 0.9	NiCrAlY (0.1 mm by APS)	S50C
8YSZ-D	8YSZ (dense)	PS(b) in Ar	0.6	NiCrAlY (0.1 mm by APS)	S50C
WA	White alumina	APS	0.6	NiCrAlY (0.1 mm by APS)	S50C
AT	Alumina-Titania	APS	0.6	NiCrAlY (0.1 mm by APS)	S50C
Metal					
NiCr/SS400	Ni20Cr	APS	0.3, 0.6	…	SS400
NiCr/SS400R	Ni20Cr	APS	0.6	…	SS400 (Rough interface)
NiCr/SKD11	Ni20Cr	APS	0.3	…	SKD11
NiCr/A5052	Ni20Cr	APS	0.3	…	A5052
NiCr/A7075	Ni20Cr	APS	0.3	…	A7075

(a) Atmospheric plasma spraying, (b) plasma spraying

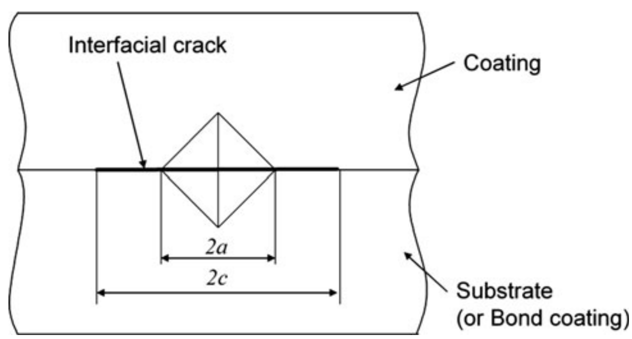

Fig. 2 Geometry of the interfacial crack induced by indentation testing

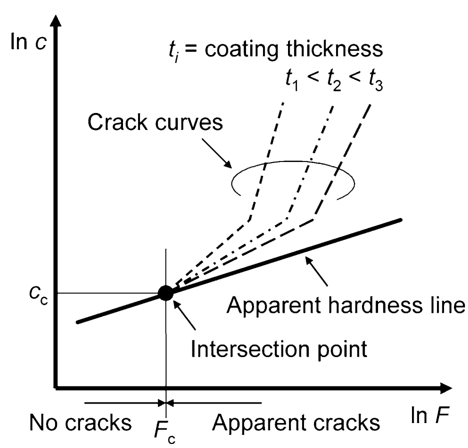

Fig. 3 Schematic illustration of crack length (c) and test force (F) on a logarithmic scale (12)

the value of P_c; the indentations must be performed from three to six load conditions to obtain the crack curve, and five indentations are needed at each load level to determine a reliable mean crack length. This is not convenient for many users, such as those at working coating-job shops, where they evaluate the interfacial fracture toughness of coatings from a few tests.

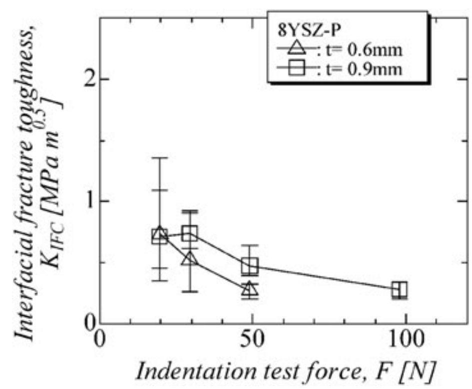

Fig. 4 Interfacial fracture toughness evaluated by Eq 1 as a function of test force

The Lesage and Chicot method can be simplified by substituting the measured crack lengths with a certain load for Eq 1 directly. Figure 4 shows typical results of the interfacial fracture toughness evaluated by Eq 1 with the (F, c) couples, which were obtained in the round-robin test. By this method, the evaluated interfacial fracture toughness varied with the test force, F. It has been also reported in Ref 19 that this value depends on the test force.

Other formulae to express interfacial fracture toughness have also been proposed (Ref 19-24). We compared some formulae to express interfacial fracture toughness from the load-dependence perspective of the test results (Ref 25). On the basis of the comparison, interfacial fracture toughness, K_{IFC}, is best expressed by the following equation:

$$K_{IFC} = \frac{A}{\sqrt{2\pi}} \frac{F}{a\sqrt{c}} \cosh(\pi\varepsilon), \quad \text{(Eq 3)}$$

where c is the crack length, a is the half-length of the impression, and A is dimensionless constant ($A = 0.081$, as determined in this study). Also, the bimaterial constant ε is defined as follows:

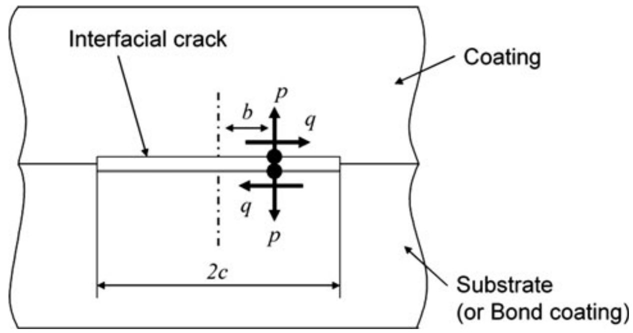

Fig. 5 Two-dimensional model of an interfacial crack subjected to mixed-mode loading

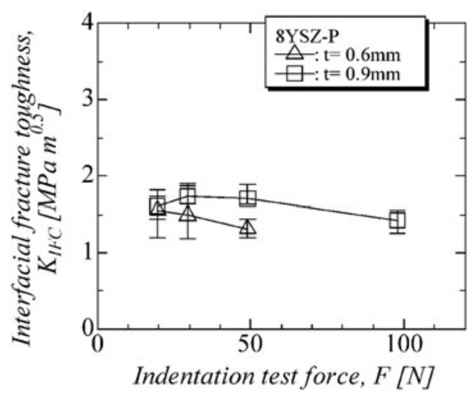

Fig. 6 Interfacial fracture toughness evaluated by Eq 3 as a function of test force

$$\varepsilon = \frac{1}{2\pi} \ln\left(\frac{\kappa_s/\mu_c + 1/\mu_s}{\kappa_c/\mu_s + 1/\mu_c}\right), \quad \text{(Eq 4)}$$

where $\kappa_i = (3 - \nu_i)/(1 + \nu_i)$; μ_i is the lateral modulus; ν_i is the Poisson's ratio; and the subscripts s and c denote substrate and coating, respectively. Equation 3 was proposed by Arai on the basis of interfacial fracture mechanics (Ref 19, 20). Arai introduced the complex stress intensity factor for evaluating the interfacial fracture toughness from an indentation test. This was done under the assumption that the internal crack geometry induced by indentation is semi-elliptical, spread along the specimen surface, as shown in Fig. 5. When the interfacial fracture toughness is evaluated by Eq 3 with the data obtained from the present round-robin tests, indentation force shows little dependence on interfacial fracture toughness, as shown in Fig. 6.

Arai reported that the crack induced in TBC specimens by indentation is semi-elliptical, similar to a Palmqvist crack (Ref 19). Equation 1 was developed on the assumption that the crack has a semicircular ''half penny'' shape. The crack shape induced in a ceramic coating might be related to the load dependence of Eq 1.

The dimensionless constant (A) in Eq 3 can be obtained from the comparison of test results of the indentation and

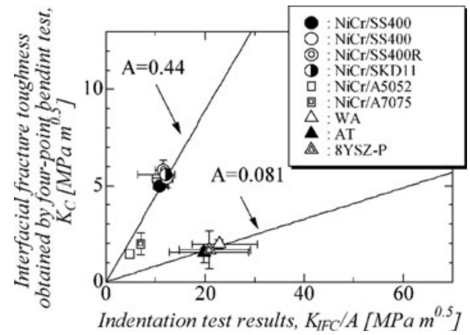

Fig. 7 Comparison of the results of indentation and four-point bending tests

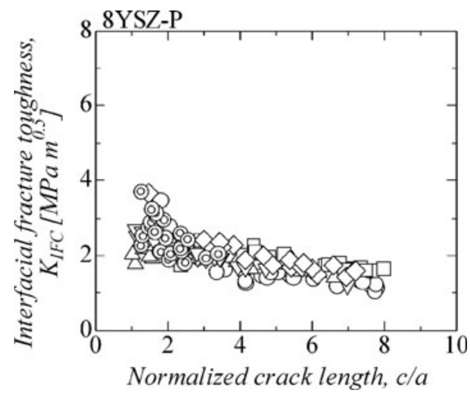

Fig. 8 Influence of crack length on the indentation interfacial toughness

other tests. Here A in Eq 3 was determined by comparing the results of indentation and four-point bending tests (Ref 26), as shown in Fig. 7. Figure 7 reveals that the results can be divided into two groups, metal and ceramic coatings. Therefore, the value of A is different for each group. By means of the least-squares approximation method, the values of A for the ceramic and metal coatings were determines as 0.081 and 0.44, respectively.

It seems that the different A values of ceramic and metallic coatings are related to the different shapes and crack propagation paths induced by the indentation. Equation 3 was defined on the basis of the interfacial cracking model, and the dimensionless constant depended on the crack shape (Ref 19). The experimental result also indicated that the cracking path in ceramic coatings induced by indentation differed from those in metallic coatings; in ceramic coatings, the crack propagated near and along the interface, whereas in metal coatings, it propagated at the interface.

4. Results and Discussions

Figure 8 shows the relationship between the indentation interfacial toughness and crack length, normalized by the half length of the impression. The indentation

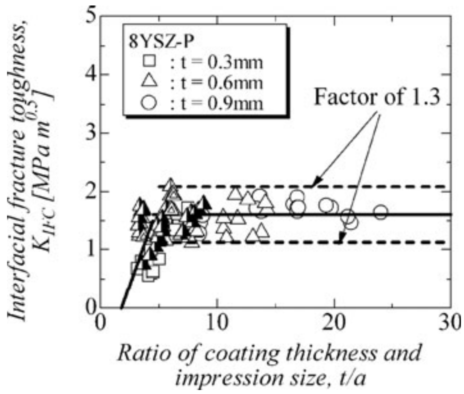

Fig. 9 Influence of coating thickness on indentation interfacial toughness

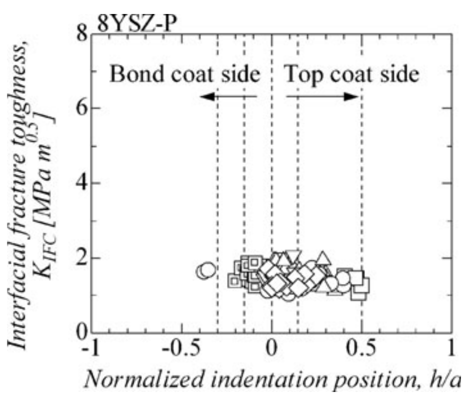

Fig. 10 Influence of the distance between the impression and the interface on the indentation interfacial toughness

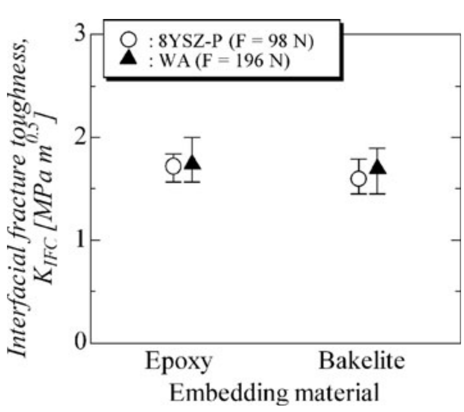

Fig. 11 Influence of the resin type on the indentation interfacial toughness

interfacial toughness decreases with crack length and approaches the intrinsic fracture resistance with the interface of the coatings.

Figure 9 indicates the influence of coating thickness, normalized by the half length of the impression, on indentation interfacial toughness, which corresponds to the intrinsic fracture toughness shown in Fig. 9. This result

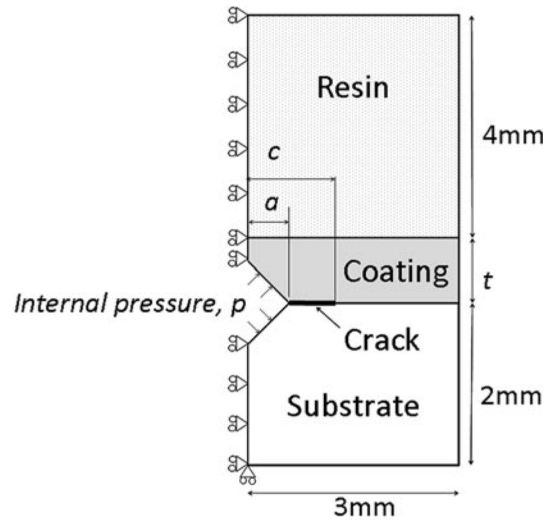

Fig. 12 Two-dimensional model used in the FE analysis

Table 2 Material constants used in the FE analysis

Material	Young's modulus (*E*), GPa
Coating	
8YSZ	20
Ni20Cr	100
Substrate	
Steel	200
Resin	
Epoxy resin	5
Phenol resin	10
Without embedding (free sample)	0

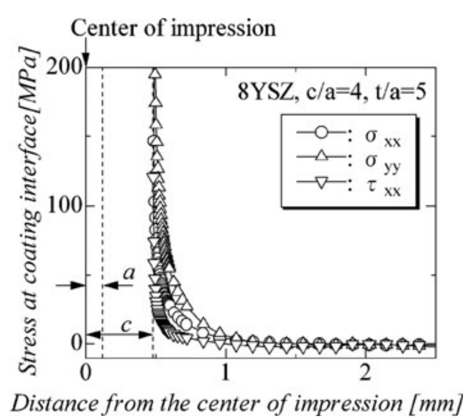

Fig. 13 Stress distribution near the crack tip induced by indentation loading

shows that the prepared sample must have sufficient thickness. When the coating thickness is five times larger than the half length of impression, the interfacial toughness is independent of the coating thickness. The effects of the ratio of indentation depth (d) and the coating thickness, d/t, have been discussed, and the so-called 1/10-rule is accepted. The ratio of the half-length and depth of impression (a/t) is 3.49 for a Vickers indenter. From this relation, $t/d = 1/10$ means $a/t \approx 1/3$; $t/a = 5$ means $d/t = 17.5$.

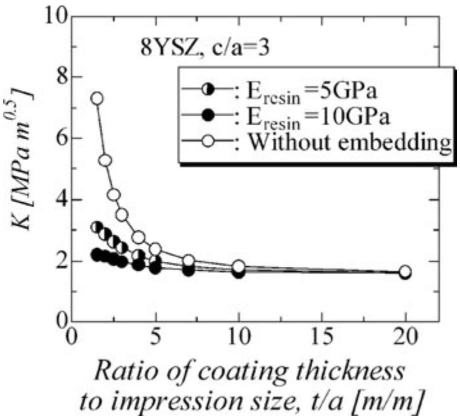

Fig. 14 Influence of resin molding on indentation interfacial toughness

Although the tip of the Vickers indenter must be placed on an interface for precise evaluation of the indentation interfacial toughness, in reality, it is difficult. Figure 10 indicates the influence of the distance between the center of impression and the interface (h) on the indentation interfacial toughness. Even when the center of impression was shifted to the ceramic coating side within the half length, the indentation interfacial toughness remained relatively unchanged.

Figure 11 shows the influence of the resin on the measured interfacial toughness. It shows that the resin rigidity has a negligible influence on the measured interfacial toughness.

The FE analysis was conducted to examine the influences of coating thickness and resin rigidity on the interfacial fracture toughness. An elastic FE analysis was performed using a two-dimensional model by subjecting the interfacial crack to an internal pressure, as shown in

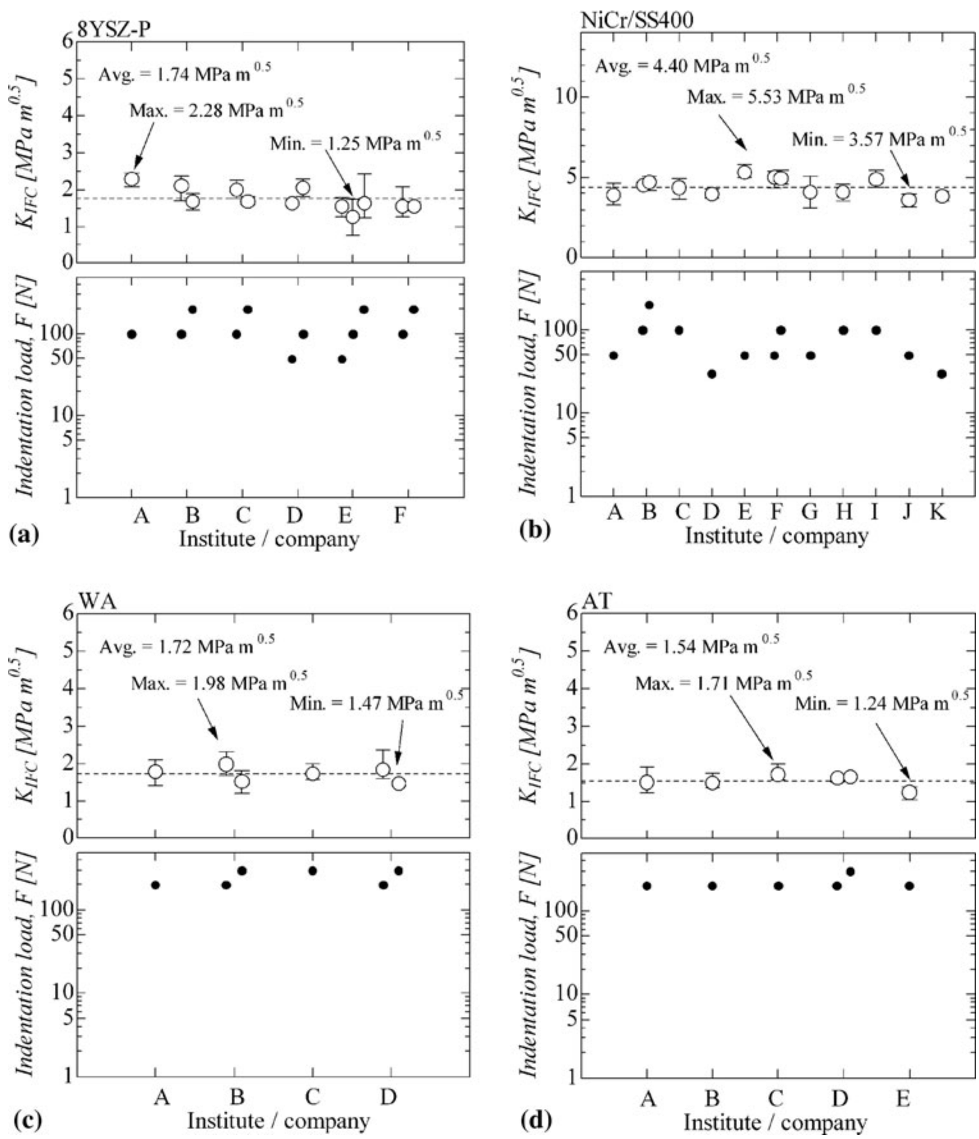

Fig. 15 Comparison of the evaluated results among collaborators

Peer Reviewed

Fig. 12. The total number of nodes was in the range of 21000-36000 (depending on the coating thickness). The material constants are listed in Table 2. In this study, the stress intensity factor at the crack tip (K) was evaluated by a stress extrapolation method from the stress distribution near the crack tip obtained by the FE analysis. From the FE analysis, it was revealed that K was proportional to the internal pressure, p. In the FE analysis, the value of p was set so that the value of K for the thick coating ($t/a = 20$) would be equal to the intrinsic interfacial toughness of the coatings, which was evaluated by the four-point bending test. For example, the condition $p = 230$ MPa was selected for $c/a = 3$ for the 8YSZ coating, which had an interfacial fracture toughness of $K_c = 1.66$ MPa m$^{0.5}$.

Typical results from the FE analyses are shown in Fig. 13 and 14. Figure 13 shows a typical stress distribution at the interface (coating side) near the crack induced by indentation. All stress components at the interface become almost zero when the distance from the crack tip exceeds 1 mm. It was observed that the interaction between cracks initiated from the impressions becomes negligible when the distance between the impressions exceeds 3 mm. Figure 14 shows the influences of the coating thickness, normalized by the half length of impression, on the stress intensity factor. The stress intensity factor approaches a constant value when the coating thickness is large; however, for thinner coatings, the stress intensity factor for the FE model without resins became larger than those with resins. This result ensures that the coating thickness was suitable for the evaluation of interfacial fracture toughness and that the resin did not affect the results.

Finally, we compared the collaborators on the basis of the evaluation results using a sample with the described geometry conditions, as shown in Fig. 15. The graphs include the indentation interfacial toughness and indentation load on the vertical axis. These results show only small amount of scattering of the indentation interfacial toughness values measured by each collaborator; no differences were observed among the collaborators.

Through the above investigations, we can evaluate the interfacial fracture toughness using the indentation test under the following conditions:

(a) The crack length must be at least three times the half-length of the impression. If it is lesser, the test must be performed again at larger indentation force to generate larger cracks.
(b) The coating thickness must be at least three times (optimally five times) the half-length of the impression.
(c) The test must be performed with the indenter tip at or near the interface. It is recommended that the distance between the center of the impression and the interface should be less than 15% of the half length of the impression.
(d) The distance between the center of any impression and the edge of the sample must be at least 3 mm.
(e) The coated samples must be embedded in the resin as test pieces to prevent damage due to polishing as well as to reduce the effect of coating thickness.

5. Conclusion

In this article, we introduced a collaborative study to evaluate the interfacial fracture toughness of thermal spray coatings using an indentation test method. Through the results of a round-robin test and FE analyses, suitable test conditions such as specimen geometry were identified for determining the interfacial fracture toughness by the indentation test. Interfacial fracture toughness values with a small amount of scatter were obtained from the indentation tests under the recommended test conditions, performed by different collaborators. Currently, we are preparing documentations for the described round-robin tests and analysis for submission to the ISO organization to recommend the technique as a new standard method.

6. Future Work

The interfacial fracture toughness evaluated by the proposed method might be affected by the residual stress (Ref 15-18), and this issue should be investigated. In the present study, FE analysis was conducted using the two-dimensional model. However, three-dimensional FE analysis should be performed with the indentation model to investigate the influences of the crack shape as well as the residual stress on the interfacial fracture toughness.

Acknowledgment

This study has been performed as collaborative research organized by the Committee on Standard Development in the Japan Thermal Spray Society. The authors express their gratitude to the committee members for their fruitful contributions. Y. Yamazaki expresses his gratitude to the New Energy and Industrial Technology Development Organization (NEDO) for partial financial support for this project.

References

1. B.R. Lawn, A.G. Evans, and D.B. Marshall, Elastic/Plastic Indentation Damage in Ceramics: The Median/Radial Crack System, *J. Am. Ceram. Soc.*, 1980, **63**, p 574-581
2. G.R. Anstis, P. Chantikul, B.R. Lawn, and D.B. Marshall, A Critical Evaluation of Indentation Techniques for Measuring Fracture Toughness: I, Direct Crack Measurements, *J. Am. Ceram. Soc.*, 1981, **64**, p 533-538
3. K. Niihara, A Fracture Mechanics Analysis of Indentation-Induced Palmqvist Crack in Ceramics, *J. Mater. Sci. Lett.*, 1983, **2**, p 221-223
4. D.B. Marshall, Controlled Flows in Ceramics: A Comparison of Knoop and Vickers Indentation, *J. Am. Ceram. Soc.*, 1983, **66**, p 127-131

5. K. Shetty, I.G. Wright, P.N. Miner, and A.H. Clauer, Indentation Fracture of WC-Co Cermets, *J. Mater. Sci.*, 1985, **20**, p 1873-1882
6. K. Tanaka, Elastic/Plastic Indentation Hardness and Indentation Fracture Toughness: The Inclusion Core Model, *J. Mater. Sci. Lett.*, 1987, **22**, p 1501-1508
7. C.B. Poton and R.D. Rawlings, Vickers Indentation Fracture Toughness test Part 1: Review of Literature and Formulation of Standardised Toughness Equations, *Mater. Sci. Technol.*, 1989, **5**, p 865-872
8. G.A. Gogotsi, S.N. Dub, E.E. Lomonova, and B.I. Ozersky, Vickers and Knoop Indentation Behaviour of Cubic and Partially Stabilized Zirconia Crystals, *J. Eur. Ceram. Soc.*, 1995, **15**, p 405-413
9. J. Gong, Indentation Toughness of Ceramics: A Statistical Analysis, *Ceram. Int.*, 2002, **28**, p 767-772
10. D. Chicot, A. Pertuz, F. Roudet, M.H. Staia, and J. Lesage, New Developments for Fracture Toughness Determination by Vickers Indentation, *Mater. Sci. Technol.*, 2004, **20**, p 877-884
11. D. Choulier, Contribution à l'étude de l'adhérence de revêtements projetés à la torche à plasma. Modélisation et utilisation d'un test d'indentation à l'interface, Thèse de doctorat, Université de Technologie de Compiègne, 1989
12. D. Chicot, P. Dèmarècaux, and J. Lesage, Apparent Interface Toughness of Substrate and Coating Couples from Indentation Test, *Thin Solid Films*, 1996, **283**, p 151-157
13. P. Demarecaux, D. Chicot, and J. Lesage, Interface Indentation Test for the Determination of Adhesive Properties of Thermal Sprayed Coatings, *J. Mater. Sci. Lett.*, 1996, **15**, p 1377-1380
14. J. Lesage and D. Chicot, Models for Hardness and Adhesion of Coatings, *Surf. Eng.*, 1999, **15**, p 447-453
15. J. Lesage and D. Chicot, Role of Residual Stress on Interface Toughness of Thermally Sprayed Coatings, *Thin Solid Films*, 2002, **415**, p 143-150
16. D. Chicot, P. Araujo, N. Horny, A. Tricoteaux, and J. Lesage, Application of the Interfacial Indentation Test for Adhesion Toughness Determination, *Surf. Coat. Technol.*, 2005, **200**, p 174-177
17. P. Araujo, D. Chicot, M. Staia, and J. Lesage, Residual Stresses and Adhesion of Thermal Spray Coatings, *Surf. Eng.*, 2005, **21**, p 1-6
18. D. Chicot, G. Marot, P. Araujo, N. Horny, A. Tricoteaux, M.H. Staia, and J. Lesage, Effect of Some Thermal Treatments on Interface Adhesion Toughness of Various Thick Thermal Spray Coatings, *Surf. Eng.*, 2006, **22**, p 390-398
19. M. Arai, Interfacial Fracture Toughness Evaluation of Ceramic Thermal Barrier Coatings Based on Indentation Test Method, *J. Soc. Mater. Sci. Jpn.*, 2009, **58**, p 917-923 (in Japanese)
20. M. Arai, Interfacial Fracture Toughness Evaluation of Thermal Barrier Coatings by Indentation Test Method, *Proceedings of Asian Pacific Conference for Materials an Mechanics* 2009, Yokohama, Japan
21. A.N. Khan, J. Lu, and H. Liao, Heat Treatment of Thermal Barrier Coatings, *Mater. Eng.*, 2003, **A359**, p 129-136
22. Y. Yamazaki, S. Kuga, and T. Yoshida, Evaluation of Interfacial Strength by an Instrumented Indentation Method and Its Application to an Actual TBC Vane, *Acta Metall. Sin.*, 2011, **24**, p 109-117
23. Y. Yamazaki and S. Kuga, Interfacial Fracture Toughness Evaluation of Thermal Barrier Coating by Instrumented Indentation Method, *Metall. J.*, 2010, **63**, p 194-200
24. R. Dal Maschio, V.M. Sglavo, L. Mattivi, L. Bertamini, and S. Sturlese, Indentation Method for Fracture Resistance Determination of Metal/Ceramic Interface in Thick TBCs, *J. Therm. Spray Technol.*, 1994, **3**, p 51-56
25. Y. Yamazaki, M. Suzuki, M. Arai, Y. Miyashita, and H. Waki, Current Activities for Standardization on Indentation Method to Evaluate Adhesion Strength of Thermal Spray Coatings in Japan, *Proceeding of the ITSC2013 ''International Thermal Spray Conference and Exposition 2013''*, May 13, 2013, Republic of Korea, Busan, 2013
26. Y. Yamazaki, A. Schmidt, and A. Scholz, The Determination of the Delamination Resistance in Thermal Barrier Coatings by Four-Point Bending Tests, *Surf. Coat. Technol.*, 2006, **201**, p 744-754

Peer Reviewed